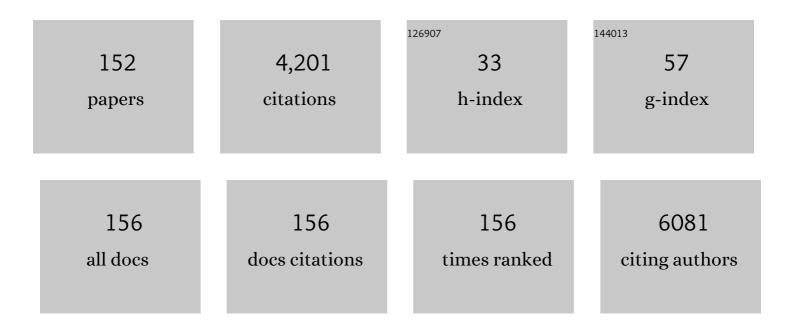


List of Publications by Year in descending order

Source: https://exaly.com/author-pdf/899323/publications.pdf Version: 2024-02-01



יוארים

#	Article	IF	CITATIONS
1	Dualâ€Design of Nanoporous to Compact Interface via Atomic/Molecular Layer Deposition Enabling a Long‣ife Silicon Anode. Advanced Functional Materials, 2022, 32, 2109682.	14.9	26
2	An umpolung strategy for rapid access to thermally activated delayed fluorescence (TADF) materials based on phenazine. Chemical Communications, 2022, 58, 1581-1584.	4.1	6
3	Probing oil recovery in shale nanopores with small-angle and ultra-small-angle neutron scattering. International Journal of Coal Geology, 2022, 253, 103950.	5.0	5
4	Hosting AlCl3 on ternary metal oxide composites for catalytic oligomerization of 1-decene: Revealing the role of supports via performance evaluation and DFT calculation. Microporous and Mesoporous Materials, 2022, 333, 111665.	4.4	2
5	Tip-Induced In-Plane Ferroelectric Superstructure in Zigzag-Wrinkled BaTiO ₃ Thin Films. Nano Letters, 2022, 22, 2859-2866.	9.1	11
6	Elucidating the promoting role of Mo2C in methane activation using Ni-xMo2C/FAU to catalyze methane steam reforming. Applied Catalysis B: Environmental, 2022, 310, 121250.	20.2	13
7	4D Printing of a Fully Biobased Shape Memory Copolyester <i>via</i> a UV-Assisted FDM Strategy. ACS Sustainable Chemistry and Engineering, 2022, 10, 6304-6312.	6.7	14
8	Machine-learning-guided reaction kinetics prediction towards solvent identification for chemical absorption of carbonyl sulfide. Chemical Engineering Journal, 2022, 444, 136662.	12.7	8
9	Reversible ionic liquids (RevILs) for the preparation of thermally stable SBA-15 supported gold nanoparticle catalysts. Applied Catalysis A: General, 2022, 643, 118725.	4.3	1
10	Constructing AgY@Cu-BTC hybrid composite for enhanced sulfides capture and moisture resistance. Microporous and Mesoporous Materials, 2022, 341, 112043.	4.4	2
11	Determining the hydration energetics on carbon-supported Ru catalysts: An adsorption calorimetry and density functional theory study. Catalysis Today, 2021, 365, 172-180.	4.4	3
12	Band structure engineering of van der Waals heterostructures using ferroelectric clamped sandwich structures. Physical Review B, 2021, 103, .	3.2	11
13	Synthesis of Imidazole-Based [30]Heptaphyrin and Stable Figure-Eight [60]Tetradecaphyrins via [5 + 2] Condensations in One Pot. Organic Letters, 2021, 23, 3746-3750.	4.6	9
14	Strain Control of Phase Transition and Exchange Bias in Flexible Heusler Alloy Thin Films. ACS Applied Materials & Interfaces, 2021, 13, 24285-24294.	8.0	12
15	Thermodynamic, Thermal, and Structural Stability of Bimetallic MIL-53 (Al _{1–<i>x</i>} Cr _{<i>x</i>}). Journal of Physical Chemistry C, 2021, 125, 14039-14047.	3.1	10
16	Tailoring Stress and Ion-Transport Kinetics via a Molecular Layer Deposition-Induced Artificial Solid Electrolyte Interphase for Durable Silicon Composite Anodes. ACS Applied Materials & Interfaces, 2021, 13, 32520-32530.	8.0	16
17	Ultrasonic activation of inert poly(tetrafluoroethylene) enables piezocatalytic generation of reactive oxygen species. Nature Communications, 2021, 12, 3508.	12.8	153
18	Iridium(III) atalyzed Diarylation/Annulation of Benzoic Acids: Facile Access to Multiâ€Aryl Spirobifluorenes as Pure Hydrocarbon Hosts for Highâ€Performance OLEDs. Angewandte Chemie - International Edition, 2021, 60, 18852-18859.	13.8	32

#	Article	IF	CITATIONS
19	Unveiling the Interfacial and Structural Heterogeneity of Ti ₃ C ₂ T _{<i>x</i>} MXene Etched with CoF ₂ /HCl by Integrated <i>in Situ</i> Thermal Analysis. ACS Applied Materials & Interfaces, 2021, 13, 52125-52133.	8.0	10
20	Thermodynamics of molybdenum trioxide encapsulated in zeolite Y. AICHE Journal, 2021, 67, e17464.	3.6	2
21	Formation Energetics and Guest—Host Interactions of Molybdenum Carbide Confined in Zeolite Y. Industrial & Engineering Chemistry Research, 2021, 60, 13991-14003.	3.7	3
22	Realizing the enhanced cyclability of a cactus-like NiCo2O4 nanocrystal anode fabricated by molecular layer deposition. Dalton Transactions, 2021, 50, 511-519.	3.3	3
23	Spontaneous self-formation of molecular ferroelectric heterostructures. Physical Chemistry Chemical Physics, 2021, 23, 3335-3340.	2.8	1
24	Structure–Property–Energetics Relationship of Organosulfide Capture Using Cu(I)/Cu(II)-BTC Edited by Valence Engineering. Industrial & Engineering Chemistry Research, 2021, 60, 371-377.	3.7	8
25	Energetics, Interlayer Molecular Structures, and Hydration Mechanisms of Dimethyl Sulfoxide (DMSO)–Kaolinite Nanoclay Guest–Host Interactions. Journal of Physical Chemistry Letters, 2021, 12, 9973-9981.	4.6	9
26	<mml:math xmlns:mml="http://www.w3.org/1998/Math/MathML"><mml:mi>β</mml:mi></mml:math> -delayed one-neutron emission probabilities within a neural network model. Physical Review C, 2021, 104, .	2.9	7
27	Atomic-scale fatigue mechanism of ferroelectric tunnel junctions. Science Advances, 2021, 7, eabh2716.	10.3	25
28	Ferroelectric Tunnel Junctions: Modulations on the Potential Barrier. Advanced Materials, 2020, 32, e1904123.	21.0	179
29	Liquid–solid–solution synthesis of ultrafine Gd2Zr2O7 nanoparticles with yield enhancement. Ceramics International, 2020, 46, 1216-1219.	4.8	7
30	Dehydration Pathway of CoF ₂ ·4H ₂ O Revisited by Integrated ex Situ and in Situ Calorimetric and Structural Studies. Journal of Physical Chemistry C, 2020, 124, 3551-3556.	3.1	3
31	Pd(II)-Catalyzed Regioselective Multiple C–H Arylations of 1-Naphthamides with Cyclic Diaryliodonium Salts: One-Step Access to [4]- and [5]Carbohelicenes. Organic Letters, 2020, 22, 135-139.	4.6	9
32	Hydration Energetics of a Diamine-Appended Metal–Organic Framework Carbon Capture Sorbent. Journal of Physical Chemistry C, 2020, 124, 398-403.	3.1	8
33	Coexistence of Magnetic Orders in Two-Dimensional Magnet Crl ₃ . Nano Letters, 2020, 20, 553-558.	9.1	74
34	Titanicone-derived TiO ₂ quantum dot@carbon encapsulated ZnO nanorod anodes for stable lithium storage. Dalton Transactions, 2020, 49, 10866-10873.	3.3	9
35	Calculation of nuclear charge radii with a trained feed-forward neural network. Physical Review C, 2020, 102, .	2.9	39
36	Thermal Evolutions and Resulting Microstructural Changes in Kerogen-Rich Marcellus Shale. ACS Earth and Space Chemistry, 2020, 4, 2461-2469.	2.7	6

#	Article	IF	CITATIONS
37	Thermodynamics of CeSiO ₄ : Implications for Actinide Orthosilicates. Inorganic Chemistry, 2020, 59, 13174-13183.	4.0	18
38	Mesoporous silica-encapsulated gold core–shell nanoparticles for active solvent-free benzyl alcohol oxidation. Reaction Chemistry and Engineering, 2020, 5, 1939-1949.	3.7	5
39	Spin-Filtering Ferroelectric Tunnel Junctions as Multiferroic Synapses for Neuromorphic Computing. ACS Applied Materials & Interfaces, 2020, 12, 56300-56309.	8.0	37
40	High-Temperature Thermodynamics of Cerium Silicates, A-Ce ₂ Si ₂ O ₇ , and Ce _{4.67} (SiO ₄) ₃ O. ACS Earth and Space Chemistry, 2020, 4, 2129-2143.	2.7	23
41	<i>In Situ</i> Hydrothermal Conversion of Silica Gel Precursors to Binderless Zeolite X Pellets for Enhanced Olefin Adsorption. Industrial & amp; Engineering Chemistry Research, 2020, 59, 9997-10009.	3.7	8
42	Conductivity Modulation of a Slit Channel in a Monolayer MoS 2 Homostructure. Physica Status Solidi - Rapid Research Letters, 2020, 14, 2000082.	2.4	0
43	Thermodynamics of Water–Cationic Species–Framework Guest–Host Interactions within Transition Metal Ion-Exchanged Mordenite Relevant to Selective Anaerobic Oxidation of Methane to Methanol. Journal of Physical Chemistry Letters, 2020, 11, 4774-4784.	4.6	8
44	Ferroelasticâ€Domainâ€Assisted Mechanical Switching of Ferroelectric Domains in Pb(Zr,Ti)O ₃ Thin Films. Advanced Electronic Materials, 2020, 6, 2000300.	5.1	12
45	Small-angle Neutron Scattering (SANS) Characterization of Clay- and Carbonate-rich Shale at Elevated Pressures. Energy & Fuels, 2020, 34, 8178-8185.	5.1	22
46	Contributions of optimized tensor interactions on the binding energies of nuclei. Nuclear Science and Techniques/Hewuli, 2020, 31, 1.	3.4	13
47	Exchange-biased nanocomposite ferromagnetic insulator. Physical Review B, 2020, 101, .	3.2	6
48	A mechanistic study of mesoporous TiO2 nanoparticle negative electrode materials with varying crystallinity for lithium ion batteries. Journal of Materials Chemistry A, 2020, 8, 3333-3343.	10.3	32
49	He irradiationâ€induced lattice distortion and surface blistering of Gd ₂ Zr ₂ O ₇ defectâ€fluorite ceramics. Journal of the American Ceramic Society, 2020, 103, 3425-3435.	3.8	20
50	Real-time monitoring of surface acetone enolization and aldolization. Catalysis Science and Technology, 2020, 10, 935-939.	4.1	4
51	High pyroelectric performance due to ferroelectric–antiferroelectric transition near room temperature. Journal of Materials Chemistry C, 2020, 8, 7820-7827.	5.5	13
52	Copper-catalyzed remote C–H arylation of polycyclic aromatic hydrocarbons (PAHs). Beilstein Journal of Organic Chemistry, 2020, 16, 530-536.	2.2	8
53	Energetic Cost for Being "Redox-Site-Rich―in Pseudocapacitive Energy Storage with Nickel–Aluminum Layered Double Hydroxide Materials. Journal of Physical Chemistry Letters, 2020, 11, 3745-3753.	4.6	11
54	Planetary ballâ€milling of AlON powder for highly transparent ceramics. Journal of the American Ceramic Society, 2019, 102, 2377-2389.	3.8	29

#	Article	IF	CITATIONS
55	Comparison of chemical stability and corrosion resistance of group IV metal oxide films formed by thermal and plasma-enhanced atomic layer deposition. Scientific Reports, 2019, 9, 10438.	3.3	30
56	Tuning <i>n</i> -Alkane Adsorption on Mixed-Linker Zeolitic Imidazolate Framework-8-90 via Controllable Ligand Hybridization: Insight into the Confinement from an Energetics Perspective. Industrial & Engineering Chemistry Research, 2019, 58, 13274-13283.	3.7	13
57	Thermodynamics of Complex Solids. Journal of Materials Research, 2019, 34, 3241-3242.	2.6	2
58	Inhibition of AlF ₃ ·3H ₂ O Impurity Formation in Ti ₃ C ₂ T _{<i>x</i>} MXene Synthesis under a Unique CoF _{<i>x</i>} /HCl Etching Environment. ACS Applied Energy Materials, 2019, 2, 8145-8152.	5.1	39
59	Double <i>ortho</i> -C–H Activation/Annulation of Benzamides with Aryl Alkynes: A Route to Double-Helical Polycyclic Heteroaromatics. Journal of Organic Chemistry, 2019, 84, 15697-15705.	3.2	18
60	Surface energetics of carbon nanotubes–based nanocomposites fabricated by microwave-assisted approach. Journal of Materials Research, 2019, 34, 3361-3367.	2.6	4
61	Manipulating Oxidation States of Copper within Cu-BTC Using Na ₂ S ₂ O ₃ as a New Strategy for Enhanced Adsorption of Sulfide. Industrial & Engineering Chemistry Research, 2019, 58, 19503-19510.	3.7	14
62	Recent advances in experimental thermodynamics of metal–organic frameworks. Powder Diffraction, 2019, 34, 297-301.	0.2	4
63	Oxidative C–H/C–H Cross-Coupling of [1,2,4]Triazolo[1,5- <i>a</i>]pyrimidines with Indoles and Pyrroles: Discovering Excited-State Intramolecular Proton Transfer (ESIPT) Fluorophores. Organic Letters, 2019, 21, 4058-4062.	4.6	25
64	Energetics of hydration on uranium oxide and peroxide surfaces. Journal of Materials Research, 2019, 34, 3319-3325.	2.6	9
65	An unusual [4 + 2] fusion strategy to forge meso-N/O-heteroarene-fused (quinoidal) porphyrins with intense near-infrared Q-bands. Chemical Science, 2019, 10, 7274-7280.	7.4	20
66	Transient directing ligand- and solvent-controlled C–H/C–H cross-coupling/quaternization cyclization/dequaternization of benzaldehydes with thiophenes. Chemical Communications, 2019, 55, 7518-7521.	4.1	21
67	Tuning Ni/Al Ratio to Enhance Pseudocapacitive Charge Storage Properties of Nickel–Aluminum Layered Double Hydroxide. Advanced Electronic Materials, 2019, 5, 1900215.	5.1	39
68	Tuning 1-hexene/n-hexane adsorption on MOF-74 via constructing Co-Mg bimetallic frameworks. Microporous and Mesoporous Materials, 2019, 284, 151-160.	4.4	51
69	The effects of precipitants on co-precipitation synthesis of yttria-stabilized zirconia nanocrystalline powders. Journal of Sol-Gel Science and Technology, 2019, 90, 359-368.	2.4	29
70	Imaging quantum spin Hall edges in monolayer WTe ₂ . Science Advances, 2019, 5, eaat8799.	10.3	113
71	Defectâ€fluorite Gd 2 Zr 2 O 7 ceramics under helium irradiation: Amorphization, cell volume expansion, and multiâ€stage bubble formation. Journal of the American Ceramic Society, 2019, 102, 4911-4918.	3.8	24
72	Rapid preparation of dense Gd2Zr2O7 nano-grain ceramics by microwave sintering in air. Ceramics International, 2019, 45, 10930-10935.	4.8	11

#	Article	IF	CITATIONS
73	Surface morphology and microstructure evolution of B4C ceramic hollow microspheres prepared by wet coating method on a pyrolysis substrate. Ceramics International, 2019, 45, 7916-7922.	4.8	7
74	Tuning the Catalytic Activity and Stability of Al–Ti Bimetallic Species Immobilized on MgO–Al2O3–SiO2 for 1-Decene Oligomerization. Industrial & Engineering Chemistry Research, 2018, 57, 6664-6672.	3.7	7
75	Enhanced Grain Growth Behavior of Ferritic Steel during Continuous Cyclic Annealing. Steel Research International, 2018, 89, 1800222.	1.8	0
76	Oneâ€pot synthesis of binderless zeolite A spheres via <i>in situ</i> hydrothermal conversion of silica gel precursors. AICHE Journal, 2018, 64, 4027-4038.	3.6	12
77	Construction of 3,7-Dithienyl Phenothiazine-Based Organic Dyes via Multistep Direct C–H Arylation Reactions. Journal of Organic Chemistry, 2018, 83, 8114-8126.	3.2	14
78	Rapid preparation and uniformity control of B4C ceramic double-curvature shells: Aim to advance its applications as ICF capsules. Journal of Alloys and Compounds, 2018, 762, 67-72.	5.5	12
79	Pd-Catalyzed Direct C–H Functionalization/Annulation of BODIPYs with Alkynes to Access Unsymmetrical Benzo[<i>b</i>]-Fused BODIPYs: Discovery of Lysosome-Targeted Turn-On Fluorescent Probes. Journal of Organic Chemistry, 2018, 83, 9538-9546.	3.2	38
80	Fabrication and Characterization of ZnO Nano-Clips by the Polyol-Mediated Process. Nanoscale Research Letters, 2018, 13, 47.	5.7	14
81	Seeding Iron Trifluoride Nanoparticles on Reduced Graphite Oxide for Lithium-Ion Batteries with Enhanced Loading and Stability. ACS Applied Materials & Interfaces, 2018, 10, 29505-29510.	8.0	21
82	Tailoring Mesoporous γ-Al ₂ O ₃ Properties by Transition Metal Doping: A Combined Experimental and Computational Study. Chemistry of Materials, 2017, 29, 1338-1349.	6.7	52
83	Unexpected Sole Enolâ€Form Emission of 2â€{2′â€Hydroxyphenyl)oxazoles for Highly Efficient Deepâ€Blueâ€Emitting Organic Electroluminescent Devices. Advanced Functional Materials, 2017, 27, 1605245.	14.9	72
84	Structure and energetics of <scp>SiOC</scp> and <scp>SiOC</scp> â€modified carbonâ€bonded carbon fiber composites. Journal of the American Ceramic Society, 2017, 100, 3693-3702.	3.8	32
85	High-resolution characterization of multiferroic heterojunction using aberration-corrected scanning transmission electron microscopy. Applied Physics Letters, 2017, 110, .	3.3	10
86	Giant tunnelling electroresistance in metal/ferroelectric/semiconductor tunnel junctions by engineering the Schottky barrier. Nature Communications, 2017, 8, 15217.	12.8	165
87	Highâ€Performance Ruthenium Sensitizers Containing Imidazolium Counterions for Efficient Dye Sensitization in Water. ChemSusChem, 2017, 10, 2914-2921.	6.8	4
88	Probing the Energetics of Molecule–Material Interactions at Interfaces and in Nanopores. Journal of Physical Chemistry C, 2017, 121, 26141-26154.	3.1	18
89	Functionalized fullerenes for highly efficient lithium ion storage: Structure-property-performance correlation with energy implications. Nano Energy, 2017, 40, 327-335.	16.0	49
90	Synthesis of Phenalenylâ€Fused Pyrylium Cations: Divergent Câ^'H Activation/Annulation Reaction Sequence of Naphthalene Aldehydes with Alkynes. Angewandte Chemie - International Edition, 2017, 56, 13094-13098.	13.8	71

 # ARTICLE 91 Metal-Modified Cu-BTC & & amp; Engineering Cher 	Acid for Highly Enhanced Adsorption of Organosulfur Species. Industrial	IF	CITATIONS
91 Metal-Modified Cu-BTC / & amp; Engineering Cher	cid for Highly Enhanced Adsorption of Organosulfur Species Industrial		
	nistry Research, 2017, 56, 9541-9550.	3.7	33
92 Calorimetric Study of All Clay-Like MXene. Journa	kali Metal Ion (K ⁺ , Na ⁺ , Li ⁺) Exchange in a l of Physical Chemistry C, 2017, 121, 15145-15153.	3.1	31
93 Densification and grain g the European Ceramic S	growth of Gd2Zr2O7 nanoceramics during pressureless sintering. Journal of ociety, 2017, 37, 1059-1065.	5.7	39
C–H/C–H Coupling	i€Bithiazoleâ€Based Copolymers via Sequential Palladiumâ€Catalyzed C–H/C–X and Reactions. Macromolecular Rapid Communications, 2016, 37, 794-798.	3.9	23
Chemical strain-depende xmlns:mml="http://www 95 interfaces <mml:math< td=""><td>ent two-dimensional transport at <mml:math v.w3.org/1998/Math/MathML"> <mml:mrow> <mml:mi>R</mml:mi> <mml:msub> <mml:mte< td=""><td>xt>AlO<td>nml:mtext></td></td></mml:mte<></mml:msub></mml:mrow></mml:math </td></mml:math<>	ent two-dimensional transport at <mml:math v.w3.org/1998/Math/MathML"> <mml:mrow> <mml:mi>R</mml:mi> <mml:msub> <mml:mte< td=""><td>xt>AlO<td>nml:mtext></td></td></mml:mte<></mml:msub></mml:mrow></mml:math 	xt>AlO <td>nml:mtext></td>	nml:mtext>

#	Article	IF	CITATIONS
109	Unparalleled Ease of Access to a Library of Biheteroaryl Fluorophores via Oxidative Cross-Coupling Reactions: Discovery of Photostable NIR Probe for Mitochondria. Journal of the American Chemical Society, 2016, 138, 4730-4738.	13.7	181
110	U(<scp>v</scp>) in metal uranates: a combined experimental and theoretical study of MgUO ₄ , CrUO ₄ , and FeUO ₄ . Dalton Transactions, 2016, 45, 4622-4632.	3.3	45
111	Thermodynamics of solvent interaction with the metal–organic framework MOF-5. Physical Chemistry Chemical Physics, 2016, 18, 1158-1162.	2.8	30
112	The Polymerization Effect on Synthesis and Visible-Light Photocatalytic Properties of Low-Temperature β-BiNbO4 Using Nb-Citrate Precursor. Nanoscale Research Letters, 2015, 10, 457.	5.7	15
113	Rhodium(III)â€Catalyzed <i>ortho</i> â€Heteroarylation of Phenols through Internal Oxidative CH Activation: Rapid Screening of Singleâ€Molecular Whiteâ€Lightâ€Emitting Materials. Angewandte Chemie - International Edition, 2015, 54, 14008-14012.	13.8	133
114	Magnetic interactions in BiFe0.5Mn0.5O3 films and BiFeO3/BiMnO3 superlattices. Scientific Reports, 2015, 5, 9093.	3.3	40
115	Interface modulation and resistive switching evolution in Pt/NiO x /Al2O3/n+–Si structure. Applied Physics A: Materials Science and Processing, 2015, 118, 1365-1370.	2.3	2
116	Thermodynamics of Methane Adsorption on Copper HKUST-1 at Low Pressure. Journal of Physical Chemistry Letters, 2015, 6, 2439-2443.	4.6	23
117	Energy Landscape of Water and Ethanol on Silica Surfaces. Journal of Physical Chemistry C, 2015, 119, 15428-15433.	3.1	32
118	Molecular design of new organic sensitizers based on thieno[1,4]benzothiazine for dye-sensitized solar cells. RSC Advances, 2015, 5, 56865-56871.	3.6	6
119	Electromechanical Response from LaAlO ₃ /SrTiO ₃ Heterostructures. ACS Applied Materials & Interfaces, 2015, 7, 10146-10151.	8.0	13
120	Rhodium(III)â€Catalyzed <i>ortho</i> CH Heteroarylation of (Hetero)aromatic Carboxylic Acids: A Rapid and Concise Access to l€â€Conjugated Polyâ€heterocycles. Angewandte Chemie - International Edition, 2015, 54, 7167-7170.	13.8	122
121	Probing the energetics of organic–nanoparticle interactions of ethanol on calcite. Proceedings of the United States of America, 2015, 112, 5314-5318.	7.1	21
122	Novel Ruthenium Sensitizers with a Phenothiazine Conjugated Bipyridyl Ligand for High-Efficiency Dye-Sensitized Solar Cells. ACS Applied Materials & Interfaces, 2015, 7, 27831-27837.	8.0	45
123	Thermodynamics of metal-organic frameworks. Journal of Solid State Chemistry, 2015, 223, 53-58.	2.9	44
124	Synthesis of Water-Soluble Cyclen-Functionalised Fullerene C ₆₀ Derivatives. Journal of Chemical Research, 2014, 38, 251-253.	1.3	0
125	Effects of Al ₂ O ₃ phase composition on AlON powder synthesis via aluminothermic reduction and nitridation. International Journal of Materials Research, 2014, 105, 409-412.	0.3	9
126	Growth of high-density Ir nanocrystals by atomic layer deposition for nonvolatile nanocrystal memory applications. Journal of Vacuum Science and Technology B:Nanotechnology and Microelectronics, 2014, 32, 042201.	1.2	5

#	Article	IF	CITATIONS
127	Guest–host interactions of a rigid organic molecule in porous silica frameworks. Proceedings of the National Academy of Sciences of the United States of America, 2014, 111, 1720-1725.	7.1	45
128	Two-step preparation of AlON transparent ceramics with powder synthesized by aluminothermic reduction and nitridation method. Journal of Materials Research, 2014, 29, 2325-2331.	2.6	39
129	Energetics of Confinement of <i>n</i> -Hexane in Ca–Na Ion Exchanged Zeolite A. Journal of Physical Chemistry C, 2014, 118, 25590-25596.	3.1	18
130	Regioselective Decarboxylative Direct C–H Arylation of Boron Dipyrromethenes (BODIPYs) at 2,6-Positions: A Facile Access to a Diversity-Oriented BODIPY Library. Organic Letters, 2014, 16, 6080-6083.	4.6	80
131	Above-room-temperature molecular ferroelectric and fast switchable dielectric of diisopropylammonium perchlorate. Journal of Materials Chemistry C, 2014, 2, 9957-9963.	5.5	53
132	Energy landscape of self-assembled superlattices of PbSe nanocrystals. Proceedings of the National Academy of Sciences of the United States of America, 2014, 111, 9054-9057.	7.1	29
133	Resistive switching in \$\$hbox {BiFeO}_3\$\$ BiFeO 3 -based heterostructures due to ferroelectric modulation on interface Schottky barriers. Journal of Materials Science: Materials in Electronics, 2014, 25, 3251-3256.	2.2	13
134	A Comparative Study of Fibroblast Behaviors under Cyclic Stress Stimulus and Static Culture on 3D Patterned Matrix. Journal of Bionic Engineering, 2013, 10, 148-155.	5.0	3
135	Small molecule – Silica interactions in porous silica structures. Geochimica Et Cosmochimica Acta, 2013, 109, 38-50.	3.9	35
136	Direct Calorimetric Measurement of Enthalpy of Adsorption of Carbon Dioxide on CD-MOF-2, a Green Metal–Organic Framework. Journal of the American Chemical Society, 2013, 135, 6790-6793.	13.7	140
137	Low-temperature synthesis of K0.5FeF3 with tunable exchange bias. Applied Physics Letters, 2013, 103, 102405.	3.3	5
138	Regioselective Synthesis of 2- and 3-Substituted Imidazo[1,2- <i>a</i>]pyridines. Journal of Chemical Research, 2012, 36, 687-690.	1.3	12
139	The ferromagnetic and ferroelectric properties of (Bi _{0.9} La _{0.1})(Fe _{0.95} Co _{0.05})O ₃ . Physica Status Solidi C: Current Topics in Solid State Physics, 2012, 9, 133-136.	0.8	0
140	Forming-Free Unipolar Resistive Switching in BiFe0.95Co0.05O3 Films. Journal of Superconductivity and Novel Magnetism, 2012, 25, 1679-1682.	1.8	1
141	Room temperature ferromagnetism in ZnO prepared by microemulsion. AlP Advances, 2011, 1, 032127.	1.3	11
142	The Multiferroic Properties of (Bi0.9Ba0.1)(Fe0.95Mn0.05)O3 Films. Journal of Superconductivity and Novel Magnetism, 2011, 24, 1497-1500.	1.8	5
143	Room Temperature Multiferroicity in Zn0.98Cu0.02O Film Prepared in N Plasma. Journal of Superconductivity and Novel Magnetism, 2011, 24, 2119-2122.	1.8	0
144	Synthesis of Pyrido[1,2â€ <i>a</i>]benzimidazoles through a Copperâ€Catalyzed Cascade C–N Coupling Process. European Journal of Organic Chemistry, 2011, 2011, 5242-5245.	2.4	60

#	Article	IF	CITATIONS
145	Catalytic Alkynylation Coupling Reactions by Copper(II) Complex in Water and Its Applications to Domino Synthesis of 2â€Arylindoles. European Journal of Organic Chemistry, 2010, 2010, 5560-5562.	2.4	28
146	The ferromagnetic and ferroelectric properties of (Bi <inf>0.9</inf> La <inf>0.1</inf>)(Fe <inf>0.95</inf> Co <inf>0.05</inf>)O <inf>3</inf> . , 2010, , .		0
147	Preparation of (1â^x%)(Na0.5Bi0.5)TiO3–x%SrTiO3 thin films by a sol–gel method for dielectric tunable applications. Journal of Sol-Gel Science and Technology, 2009, 49, 29-34.	2.4	28
148	Preparation and Characterization of Relaxor Ferroelectric 0.65Pb(Mg _{1/3} Nb _{2/3})O ₃ –0.35PbTiO ₃ by a Polymerizable Complex Method. Journal of the American Ceramic Society, 2009, 92, 1256-1261.	3.8	19
149	CHEMICAL VAPOR DEPOSITION OF Zr _x Hf _{1-x} O ₂ THIN FILMS USING ANHYDROUS MIXED-METAL NITRATES PRECURSORS. Integrated Ferroelectrics, 2008, 97, 93-102.	0.7	2
150	Structure, optical, and magnetic properties of sputtered manganese and nitrogen-codoped ZnO films. Applied Physics Letters, 2006, 88, 082111.	3.3	71
151	Growth and characterization of SrBi2Ta2O9thin films prepared by rapid thermal annealing. Ferroelectrics, 2001, 263, 303-308.	0.6	0
152	Rh(<scp>iii</scp>)-catalysed C–H/C–H cross-coupling of <i>S</i> -aryl sulfoximines with thiophenes: facile access to [1]benzothieno[3,2- <i>b</i>][1]benzothiophene (BTBT) and benzothiazines. Chemical	4.1	2

Communications, 0, , .